Indian J Phys (July 2014) 88(7):665–670
DOI 10.1007/s12648-014-0471-0

ORIGINAL PAPER

Effect of site selection on dielectric properties of Fe doped $CaCu_3Ti_4O_{12}$ electro-ceramic synthesized by citrate nitrate gel route

L Singh[1], K D Mandal[2]*, U S Rai[1] and A K Rai[3]

[1]Department of Chemistry, Faculty of Science, Centre of Advanced Study, Banaras Hindu University, Varanasi 221005, Uttar Pradesh, India

[2]Department of Applied Chemistry, Indian Institute of Technology, Banaras Hindu University, Varanasi 221005, Uttar Pradesh, India

[3]Department of Materials Science and Engineering, Chonnam National University, 300 Yongbong–dong, Bukgu, Kwangju 500–757, Republic of Korea

Received: 24 October 2013 / Accepted: 24 February 2014 / Published online: 29 March 2014

Abstract: The effect of doping of Fe at Cu^{2+} and Ti^{4+} sites in calcium copper titanate, $CaCu_3Ti_4O_{12}$, has been examined. The compositions $CaCu_{3-x}Fe_xTi_4O_{12}$ (CCFTO) and $CaCu_3Ti_{4-x}Fe_xO_{12}$ (CCTFO), (x = 0.10) have been synthesized by citrate nitrate gel route. XRD analysis confirms the formation of single- phase ceramics on sintering at 900 °C for 8 h. Structure of $CaCu_3Ti_4O_{12}$ does not change on doping with iron on Cu-site or Ti-site and it remains cubic. Surface morphology indicates that the average grain size is in range of 30–90 μm and 5–7 μm for systems CCFTO and CCTFO, respectively. EDX studies confirm the presence of Ca^{2+}, Cu^{2+}, Ti^{4+} and Fe^{3+} ions as per stoichiometry of ceramics. The grain resistance of CCTFO is higher than that of CCFTO. Values of dielectric constant (ε_r) and dielectric loss ($tan\delta$) of CCTFO are higher than those of CCFTO ceramic at all measured frequencies and temperatures.

Keywords: Synthesis; Scanning electron microscopy; Materials processing; Dielectric constant

PACS Nos.: 81.05.Gc; 68.37.Hk; 81.20.Fw; 78.20.Ci

1. Introduction

Miniaturization of the microelectronics requires material of high dielectric constant (ε_r) and low dielectric loss ($tan\delta$) especially for dynamic random access memories (DRAM), capacitor and memory devices. Calcium copper titanate, $CaCu_3Ti_4O_{12}$ (CCTO), has recently attracted interest of many research workers due to its unusually high dielectric permittivity ($\varepsilon_r \sim 10^4$) which is temperature independent in the range 100–600 K [1–3]. The giant dielectric responses in CCTO is due to extrinsic mechanism caused by internal barrier layer capacitance (IBLC) associated with grain boundaries, twin boundaries, dislocation networks and Schottky barriers or interfacial polarization effect [4–6]. In CCTO, ceramic the oxygen vacancy or impurities can lead to increase in the conductivity either in bulk (grains) or at grain boundaries. Substitution effect of impurities on dielectric properties of CCTO has been reported earlier [7–10]. It is well known that radius, valancy and co-ordination number of an element are important parameters to determine the site it occupies in parent compound and the composition in range of solid solution formation [11]. In CCTO, the different metal cations have its own preferred substitution sites. The cation shows critical influence on extinction of an electrical barrier at grain boundaries and reduction of charge carriers in bulk grain. Fe^{3+} ions have been preferably substituted at Ti site rather than Cu site [12, 13]. The substitution of Fe^{3+} on Ti^{4+} site suppresses dielectric constant value by one to two orders of its magnitude and suggests that residual CuO phase and grain boundary effects are responsible for enhancement of dielectric permittivity, which is based on IBLC model. However, no evidence of microstructural changes such as grain size, CuO segregation along the grain boundary or grain [9] with doping elements has been observed.

In present study, single-phase Fe-substituted $CaCu_{3-}Ti_{4-x}Fe_xO_{12}$ and $CaCu_{3-x}Fe_xTi_4O_{12}$ (x = 0.10) ceramics, abbreviated as CCTFO and CCFTO, respectively, have been synthesized and a comparative study on electric and

*Corresponding author, E-mail: kdmandal.apc@itbhu.ac.in

dielectric properties have been reported. Impedance spectroscopy studies show that CCFTO and CCTFO are electrically homogeneous with insulating grains and insulating grain boundaries. Novel citrate nitrate gel route has been used to speed up the synthesis of complex materials at relatively lower temperature [14, 15]. It is a simple process with a significant saving of time and energy consumption compared to traditional methods such as solid state and mechanical alloying techniques. This route, employed to obtain improved powder characteristics, more homogeneity and a narrow particle size range thereby influences structural, electrical and dielectric properties of material.

2. Experimental details

$CaCu_3Ti_{4-x}Fe_xO_{12}$ and $CaCu_{3-x}Fe_xTi_4O_{12}$ (x = 0.10) were prepared by citrate nitrate gel route. Analytical grade chemicals, Ca $(NO_3)_2.4H_2O$ (99.5 %, Qualigens product), Cu $(NO_3)_2.3H_2O$ (99.9 %, Merck product), $FeSO_4(NH_4)_2SO_4.6H_2O$ (99.8 %, Ranbaxy product), TiO_2 (99.5 %, Merck product) and citric acid (99.5 %, Merck product) were used as starting materials. Standard aqueous solutions of Ca^{2+}, Cu^{2+} and Fe^{3+} were prepared in distilled water. Solutions of metal nitrates and solid TiO_2 in stoichiometric ratio were mixed in a beaker and aqueous solution of citric acid equivalent to metal ions were added to the solution. The solution was heated on a hot plate at 70–80 °C with continued stirring using a magnetic stirrer to evaporate water and dried at 100–120 °C in hot air oven for 12 h to get a blue gel. The blue gel was calcined in air at 800 °C for 6 h in an electrical furnace. Simultaneous differential thermal analysis (DTA) and thermogravimetric analysis (TGA) of dried gel were recorded using SETARAM LABSYS^{TM} TG/DTA-16, USA from 25 °C to 1,000 °C at a heating rate of 10 °C/min. The crystalline phase of the samples sintered at 900 °C for 8 h was identified using an X-ray Diffractometer (Rich-Siefert, ID-3000) employing Cu-K_α radiation. Microstructures of the fractured surfaces were examined using a scanning electron microscope (SEM, Model JEOL JSM5410). Energy dispersive X-ray analyzer (EDX, Model Kevex, Sigma KS3) was used for elemental analysis in the sintered samples. The calcined powders were ground into fine powder using a pestle and mortar. Calcined powder with 2 wt% polyvinyl alcohol (PVA) was pressed into cylindrical pellets using hydraulic press. PVA binder was burnt out at 350 °C for 2 h. Finally, pellets were sintered at 900 °C for 8 h for dielectric measurement. Sintered pellets were polished using SiC abrasive paper and diamond paste until there was a mirror finish. For the purpose of electrical measurements, silver paste was applied to both sides of the circular faces of ceramic pellet, then dried at 600 °C for 15 min and cooled naturally to room temperature. Dielectric and electrical data of CCFTO and CCTFO samples were collected using Nova controller Impedance analyzer over a frequency range 10^2–10^6 Hz and in the temperature range 300–500 K.

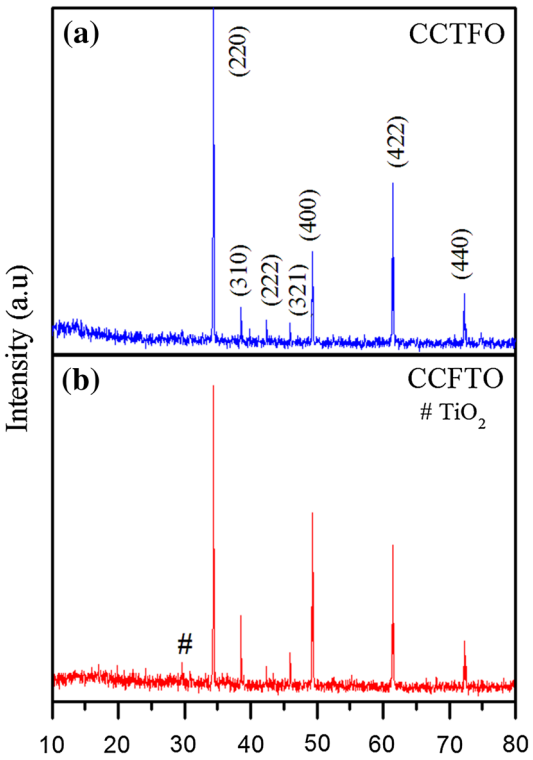

Fig. 1 X-ray powder diffraction patterns of (**a**) CCTFO and (**b**) CCFTO respectively sintered at 900 °C for 8 h

3. Result and discussion

Relative densities of CCTFO and CCFTO are 94.3 and 93.6 %, respectively. It clearly shows that density of CCTFO is higher than CCFTO. XRD patterns of the $CaCu_3Ti_{3.9}Fe_{0.1}O_{12}$ (CCTFO) and $CaCu_{2.9}Fe_{0.1}Ti_4O_{12}$ (CCFTO) ceramics sintered for 8 h at 900 °C are shown in Fig.1a and 1b respectively. It is evident that XRD patterns of the CCTFO and CCFTO samples are in good agreement with un-doped CCTO (JCPDS75-2188) and confirm the formation of major phase of CCTO while CCFTO shows minor secondary phase of TiO_2. As expected, pure CCTO phase is obtained only when the ratio of calcium, copper and titanium are very close to stoichiometric ones. It is also reported that Ti content mostly controls the phase composition (single or multi-phased material) of CCTO powder [16]. Presence of TiO_2 secondary phase in CCFTO confirms that Fe^{3+} ion preferably substitute at the Ti site rather than Cu site in CCTO lattice. All the X-ray peaks have been indexed on basis of a cubic unit cell similar to the

Table 1 Crystal system, lattice parameter and unit cell volume for CCTFO and CCFTO

System	Crystal system	Lattice parameter (Å)	Lattice volume (Å^3)
CCTFO	Cubic	7.382 ± 0.152	402.283 ± 0.012
CCFTO	Cubic	7.379 ± 0.216	401.912 ± 0.142

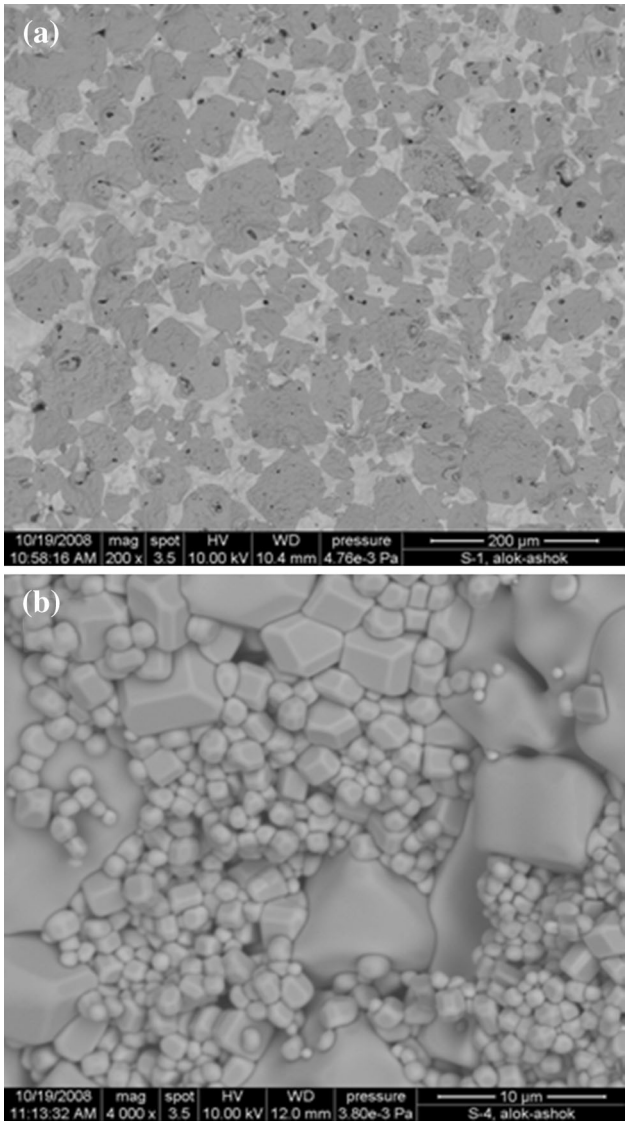

Fig. 2 SEM micrographs of (**a**) CCTFO and (**b**) CCFTO sintered at 900 °C for 8 h

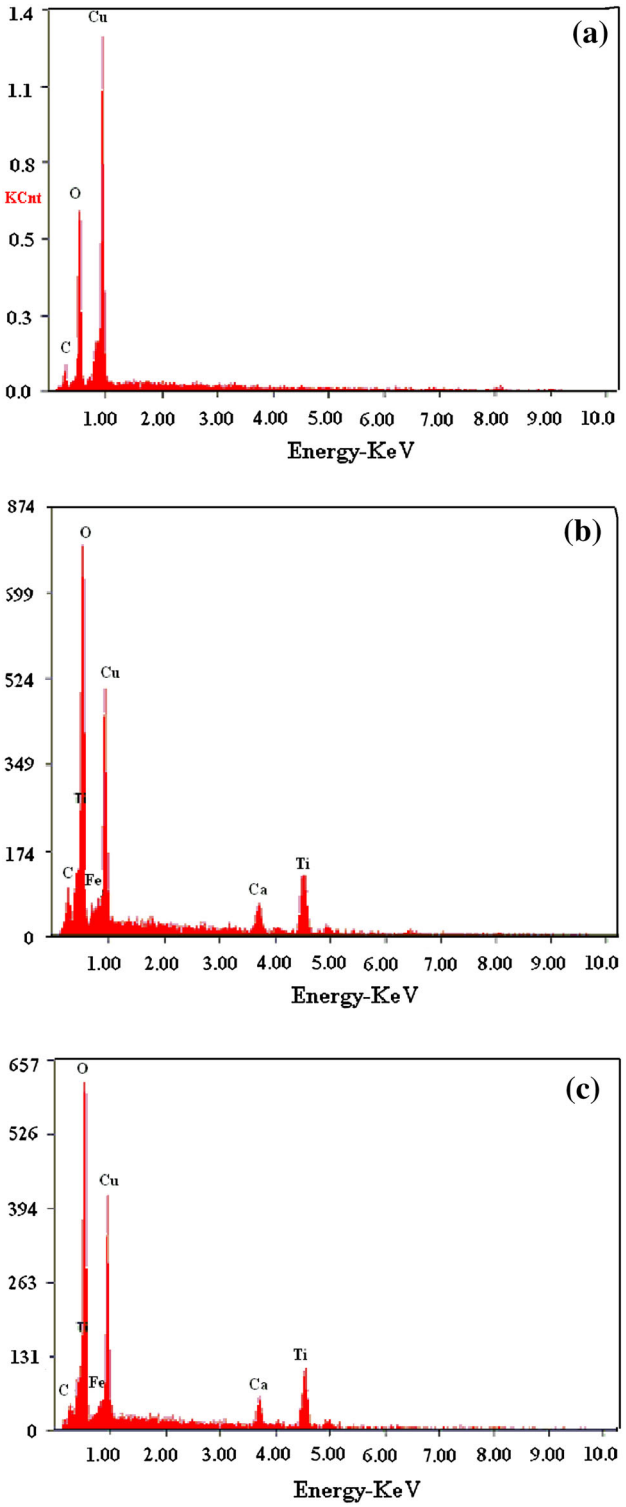

Fig. 3 EDX spectra for (**a**) CCTFO at grain (**b**) CCTFO at grain boundaries of system (**c**) CCFTO at grain of system

un-doped CCTO. Lattice parameter and unit cell volume have been determined using least square refinement method. The values of lattice parameter and unit cell volume of CCTFO and CCFTO are given in Table 1. These results show that Fe doping does not change the cubic perovskite structure. However, it causes minute increase in the unit cell volume of CCTFO due to doping of Fe^{3+} (coordination number $N = 6$, 6.45 Å) for Ti^{4+} ($N = 6$, 6.05 Å).

Figure 2(a) and 2(b) show SEM images of fractured surface of the sintered samples CCTFO and CCFTO

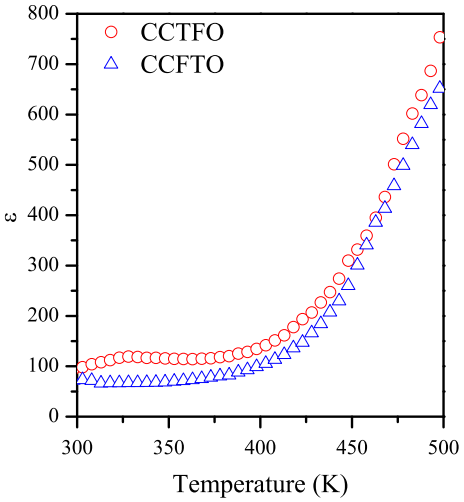

Fig. 4 Plots of dielectric constant (ε) versus temperature of CCFTO & CCTFO ceramic sintered at 900 °C for 8 h

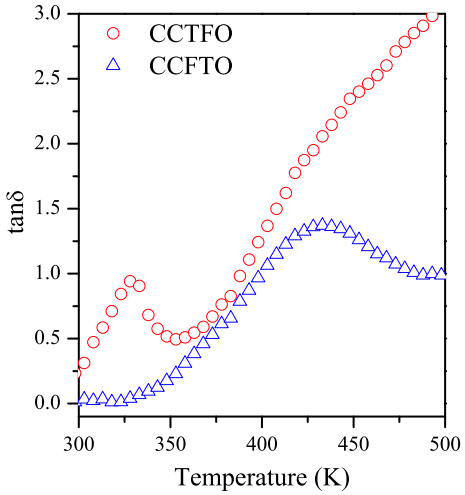

Fig. 5 Plots of dielectric loss ($tan\delta$) versus temperature of CCFTO & CCTFO ceramic sintered at 900 °C for 8 h

ceramics. Microstructure of CCTFO ceramic reveals the presence of abnormally large grains size in the range of 30–90 μm Fig. 2(a), whereas the grain size of CCFTO ceramic found to be in range of 5–7 μm. Grain size of CCFTO is smaller than that of CCTFO due to presence of secondary phase as shown in XRD patterns of Fig. 1. It is known that secondary phase can usually prohibit the movement of grain boundaries and retard grain growth in ceramics during sintering [17]. CCFTO has a few duplex microstructure consisting of a very few large grains in excess of 5–7 μm in size which are isolated by regions consisting of fine grains (1–1.5 μm). Further, the grains of CCFTO have smooth surfaces associated with a squarish appearance. Sizes of these particles synthesized by citrate nitrate gel route are relatively smaller than those prepared by other ceramic methods [18]. In case of CCTFO ceramic there is absence of agglomeration, which results abnormal grain growth. This is due to segregation of CuO at the grain boundaries of ceramic. Segregated CuO melts during sintering lead to abnormal growth [19, 20]. Presence of CuO secondary phase is confirms by EDX studies of grain boundaries. Figure 3(a)–3(c) show EDX spectra of CCTFO and CCFTO ceramics. Figure 3(a) and 3(c) clearly show the presence of Ca, Cu, Ti and Fe elements as per stoichiometric ratio in CCTFO and CCFTO ceramics and confirm purity of the materials. Figure 3(a) shows EDX of grain boundary of CCTFO ceramic which indicates presence of Cu and oxygen elements at grain-boundary. These results confirm the presence of CuO at grain-boundary.

Temperature dependence of dielectric constant (ε) for the ceramic CCFTO and CCTFO is shown in Fig. 4. It is noted in the figure that dielectric constants of CCTFO and CCFTO are $\sim$100 and 75, respectively, in room temperature and at 1 kHz. These values remain constant up to 400 K and then increases continuously with temperature. It is also observed that dielectric constant of CCTFO is more than CCFTO. This is due to formation of oxygen vacancy in CCTFO ceramic on partial substitution of Ti by the Fe^{3+} ions and small difference in density of this ceramic. Therefore, it is concluded that dielectric constant of CCTFO originated from interfacial polarization at grain boundaries [21, 22].

Figure 5 shows the variation of dielectric loss with temperature. In case of CCTFO dielectric loss peak is observed at 325 K whereas it is observed at 425 K for CCFTO ceramic. The presence of peaks in both samples of ceramic show relaxation behavior, which is attributed to the difference in microstructural features. It is also observed from Fig. 5 that dielectric loss of CCTFO ceramic is higher than that of CCFTO ceramic in temperature range of 300–500 K.

The resistance and capacitance associated with an electrically active grain and grain boundary regions in electroceramics could be estimated by impedance spectroscopy which correlates electrical behaviour of the sample to its microstructure. The simplest equivalent circuit is a series of network of three parallel RC element applied for CCTO ceramics [23]. Figure 6(a)–6(c), 6(e) and 6(g) show the Cole–Cole plots Z* (Z' vs. Z'') of CCFTO and CCTFO ceramics at 300, 350, 400, 450 and 500 K, respectively. An expanded view of impedance plane plots Z' versus Z'' at the high-frequency region close to the origin at 400, 450 and 500 K are also shown in the Right sub-graph of Fig. 6(d), 6(f) and 6(h), respectively. Two arcs are clearly observed in impedance plots for both ceramics at 350, 400, 450 and 500 K. Intercept of arc passing through origin on Z' axis gives contribution of the resistance of the grains (R_g) while that of another arc in the lower frequency range,

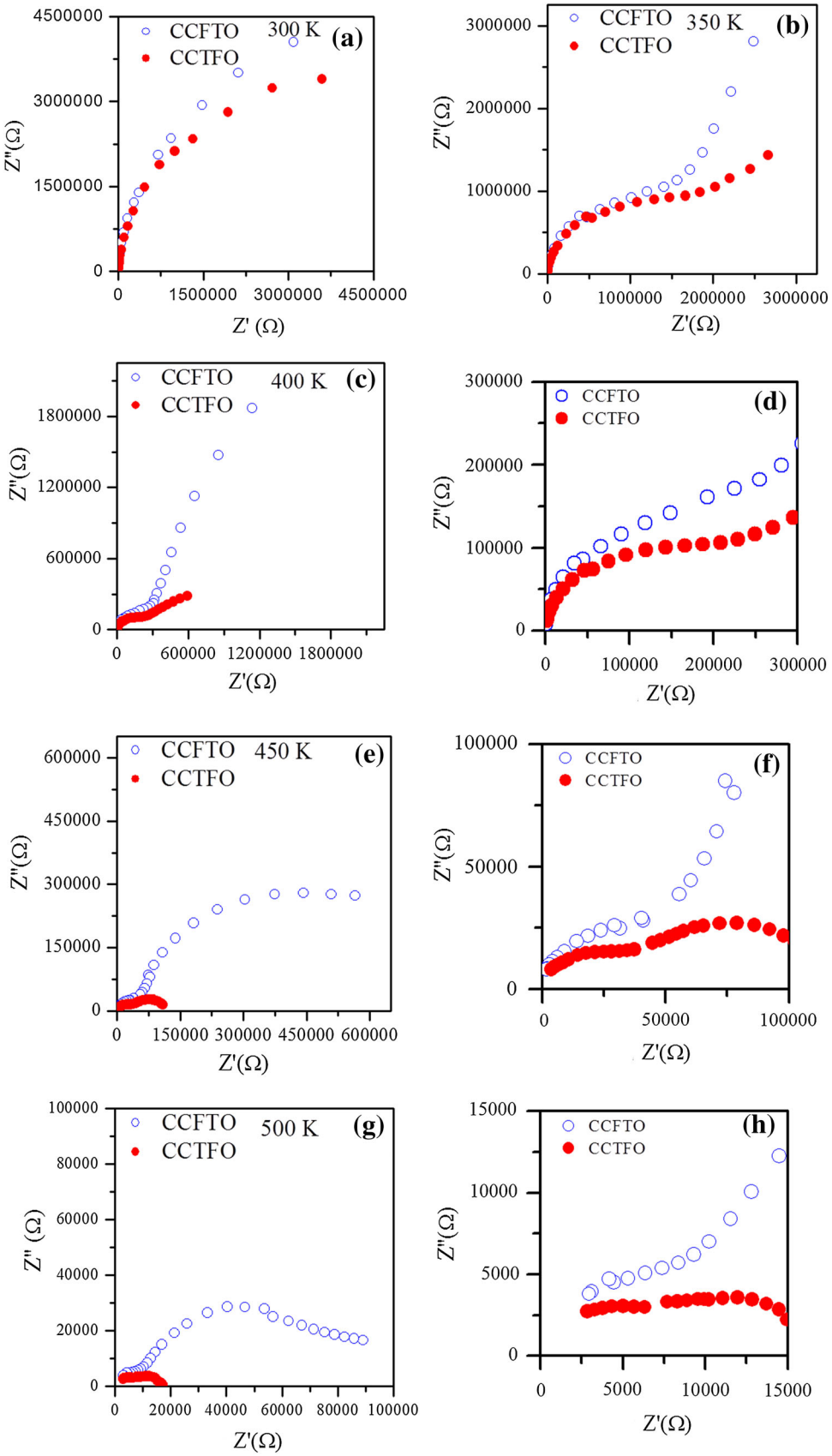

Fig. 6 Cole–Cole plots Z′ versus Z″ of CCFTO and CCTFO ceramic at temperatures (**a**) 300 K, (**b**) 350 K (**c**) 400 K (**d**) Right sub-graph: An expanded view of impedance plane plots Z′ versus, Z″ at the high-frequency region close to the origin at 400 K (**e**) 450 K (**f**) Right sub-graph: An expanded view of impedance plane plots Z′ versus Z″ at the high-frequency region close to the origin at 450 K and (**g**) 500 K (**h**) Right sub-graph: An expanded view of impedance plane plots Z′ versus Z″ at the high- frequency region close to the origin at 500 K

gives contribution of the resistance of the grain-boundaries (R_{gb}). The values of the resistance for grains (R_g) is found to be 4.18×10^4 Ω and 6.67×10^4 Ω and resistance for grain-boundaries (R_{gb}) are 1.15×10^5 Ω and 7.13×10^5 Ω for CCTFO and CCFTO ceramics, respectively. It is observed that both grains and grain-boundaries are insulating which developed electrically homogeneous structure and suppress the formation of barrier layers explaining the low value of dielectric constant in these ceramics [24, 25]. It is also observed that at 300 K, the resistance of grain is very low as compared to grain-boundary. On increasing temperature the resistance of grain and grain-boundary decreases. The Fig. 6(c)–6(e) show high frequency region impedance data. It is seen that grain and grain-boundary resistance of CCFTO ceramic is always higher than CCTFO ceramic. In large arc of CCFTO small spikes appear at low frequency end at 350 K temperature. It is clearly demonstrated in Fig. 6 that in low temperature regions, grain response is dominated whereas at higher temperature region, grain boundary responses appear with a clear semi-circle [26, 27]. CCTFO ceramic shows very clearly electrode contribution at higher temperatures. At higher temperatures grain contribution moved out from the plot. One can get a clear grain contribution towards conductivity if low temperature measurement would be performed. High conductivity of CCTFO ceramic may be due to oxygen deficiency (or vacancy) which is created on partial substitution of Ti by Fe^{3+} in CCTO ceramic.

4. Conclusions

In summary CCTFO and CCFTO ceramics have been synthesized by citrate nitrate gel route using metal nitrate solution and TiO_2 powder. While single-phase formation is confirmed by XRD, the stoichiometry of the synthesized ceramics, of CCTFO & CCFTO have been verified by EDX studies. Impedance analyses of both the ceramics show that grain boundary resistances dominate total resistance of ceramics. Dielectric- constant responses of both the ceramics arises from the space charge polarization. Resistance of grain-boundary is several orders larger than that of grain.

Acknowledgments Authors would like to thank to Prof. R K Mandal, Department of Metallurgical Engineering, IIT(Banaras Hindu University) for extending SEM facility.

References

[1] M A Subramanian, D Li, N Duan, B A Reisner and A W Sleight *J. Solid State Chem.* **151** 323 (2000)
[2] C C Homes, T Vogt, S M Shapiro, S Wakimoto and A P Ramirez *Science* **293** 673 (2001)
[3] L Chen et al. *Appl. Phys. Lett.* **82** 2317 (2003)
[4] D C Sinclair, T B Adams, F Morrison and A R West *Appl. Phys. Lett.* **80** 2153 (2002)
[5] S Aygun, X Tan, J P Maria and D P Cann *Proc 204th Electrochem. Soc. Meeting* Orlando, Florida z (2003)
[6] L He, J B Neaton, D Vanderbilt and M H Cohen *Phys. Rev. B* **67** 012103 (2003)
[7] W Kobayashi and I Terasaki *Phys. B* **771** 329 (2003)
[8] G Chiodelli et al. *Solid State Commun.* **132** 24 (2004)
[9] D Capsoni, M Bini, V Massarotti, G Chiodelli, M C Mozzati and C B Azzoni *J. Solid State Chem.* **177** 4494 (2004)
[10] M Li, A Feteira, D C Sinclair and A R West *Appl. Phys. Lett.* **88** 232903 (2006)
[11] M T Buscaglia, M Viviani, V Buscaglia and C Bottino *J. Am. Ceram. Soc.* **85** 1569 (2002)
[12] S Y Chung, S Y Choi, T Yamamoto, Y Ikuhara and S J L Kang *Appl. Phys. Lett.* **88** 091917 (2006)
[13] S Y Choi, S Y Chung, T Yamamoto and Y Ikuhara *Adv. Mater.* **21** 885 (2009)
[14] I Soibam and S Phanjoubam *Indian J. Phys.* **87** 121 (2013)
[15] A Govindan, A Sharma, A K Pandey and S K Gaur *Indian J. Phys.* **85** 1829 (2011)
[16] S G Fritsch, T Lebey, M Boulos and B Durand *J. Eur. Ceram. Soc.* **26** 1245 (2006)
[17] W H Tzing and W H Tuan *Ceram. Inter.* **25** 69 (1999)
[18] P Jha, P Arora and A K Ganguli *Mater. Lett.* **57** 2443 (2003)
[19] D W Kim, T G Kim and F S Hong *Mater. Res. Bull.* **34** 771 (1999)
[20] C L Huang and Y C Chen *Mater. Res. Bull.* **37** 563 (2002)
[21] R K Grubbs, E L Venturini, P G Clem, J J Richardson, B A Tuttle and G A Samara *Phys. Rev. B* **72** 104111 (2005)
[22] C Mu, H Zhang, Y He, J Shen and P Liu *J. Phys. D: Appl. Phys.* **42** 175410 (2009)
[23] M Mitsugi, S Asanuma, Y Uesu, M Fukunga, W Kobayashi and I Terasaki *Appl. Phys. Lett.* **90** 242904 (2007)
[24] S I R Costa, M Li, J R Frade and D C Sinclair *RSC Adv.* **3** 7030 (2013)
[25] C Mu, H Zhang, Y He and A Liu *Phys. B* **405** 386 (2010)
[26] K C V Rajulu, K S Rao, B Tilak, G Gangadharudu and A Swathi *Indian J. Phys.* **86** 625 (2012)
[27] L Fang, M Shen, F Zheng, Z Li and J Yang *J. Appl. Phys.* **104** 064110 (2008)